

## Stable elliptical vortices in a circular disk

Peilong Chen\*

*Department of Physics and Center for Complex Systems, National Central University, Chungli 320, Taiwan*

(Received 23 November 1998)

We show that large elliptical vortices in a finite disk are stable in a two-dimensional (2D) ideal fluid (this also applies to a column of quasi-2D non-neutral plasma in an axial magnetic field). The stability is established by comparison between the energy of elliptical and symmetrical states to satisfy a sufficient condition, without dynamical eigenanalysis. Analytical small ellipticity expansion of system energy and exact numerical values for arbitrary ellipticity are both obtained for uniform vortices. An approximating calculation is presented for general smooth vortices. Numerical simulations of the 2D Euler equation are also performed. The simulations not only confirm the sufficient condition, but also show that the stability persists to smaller vortex sizes. The reason why decaying  $l=2$  modes were obtained by Briggs, Daugherty, and Levy [Phys. Fluids **13**, 421 (1970)] using eigenanalysis is also discussed. [S1063-651X(99)08908-4]

PACS number(s): 47.15.Ki, 47.20.-k, 52.25.Wz

### I. INTRODUCTION

The two-dimensional (2D) incompressible Euler equation

$$\frac{\partial \omega}{\partial t} + (\mathbf{u} \cdot \nabla) \omega = 0 \quad (1)$$

not only describes an incompressible 2D ideal fluid, but also governs the behavior of a long non-neutral plasma column confined by a uniform axial magnetic field [1]. Here,  $\mathbf{u}(x, y)$  is the 2D velocity field and  $\omega(\mathbf{r})$  the vorticity field,  $\omega \equiv (\nabla \times \mathbf{u}) \cdot \hat{\mathbf{z}}$ . The incompressibility condition,  $\nabla \cdot \mathbf{u} = 0$ , can be automatically satisfied by defining the stream function  $\phi$  such as  $\mathbf{u} = (\partial \phi / \partial y, -\partial \phi / \partial x)$ . The stream function and vorticity are related by the Poisson equation  $\nabla^2 \phi = -\omega$ . In a pure electron plasma,  $\omega$  corresponds to the electron density and  $\phi$  to the electrical potential.

Stability problems of coherent vortex states in this system have long been interesting and important questions. In a free space, there exist exact nonlinear elliptical (Kirchoff) uniform vorticity solutions [2]. In a cylindrical geometry, Briggs, Daugherty, and Levy [3] showed that, using dynamical eigenanalysis, resonance between fluid elements and wave modes will lead to damping of  $l \geq 2$  diocotron modes. Here,  $l$  denotes the mode number when the perturbation to a symmetric stream function is written as  $\phi_l(r) \exp[i(\Omega t - l\theta)]$ . By solving the initial value problem of linearized dynamical equations and properly treating analytical continuation in the complex  $\Omega$  plane, they obtained a formulation for the complex eigenvalue  $\Omega$ . In particular, for a vorticity distribution very close to a step function [i.e.,  $\omega(r < r_0) = 1$  and  $\omega(r > r_0) = 0$ ] but with negative radial derivative at all places,  $\Omega$  with a positive imaginary part is calculated for  $l \geq 2$ , leading to decaying normal modes.

Experimental observations of decaying  $l=2$  modes have been performed by Pillai and Gould [4] in a pure electron plasma. Exponential decay rates were obtained, as well as

the observation of fluid trapping in the diocotron mode at large amplitudes. In another experiment with a pure electron plasma [5], beat-wave resonance damping (transitions from high  $l$  modes to low  $l$  modes) was observed to be the dominant vortex symmetrization mechanism.

A stability argument based on global constraints has also been applied to the 2D vortex system [6]. The logic of this analysis is to show that a functional  $W[\omega(\mathbf{r})]$  which is conserved by the 2D Euler equation is a maximum at a particular  $\omega(\mathbf{r})$  against all other states that are accessible under incompressible flows. At this maximum, no further changes in  $\omega(\mathbf{r})$  are possible and the state is then stable. For example, Davidson and Lund [7] showed that a state in a cylindrical geometry following a relation  $\omega(\mathbf{r}) = \omega(\phi(\mathbf{r}))$  and  $\partial \omega(\phi) / \partial \phi \geq 0$  is nonlinearly stable [8]. In another example, O'Neil and Smith [9] demonstrated that an off-center coherent vortex (linearly an  $l=1$  perturbation) in a disk is also stable. However, no results on the stability of an  $l=2$  mode using this method have been given in the literature.

Thermal equilibrium has been studied in 2D ideal fluids [10]. Since the coarse-grained entropy will not decrease due to the dynamical vorticity mixing, it is proposed that the system will reach a maximum coarse-grained entropy state at long time. Mean field equations governing these states have been derived [10], and solutions in some situations were obtained [11]. Once a mean-field equilibrium state is obtained, its stability can be assured by showing a positive second derivative of entropy against all possible perturbations. This test of stability is similar to the method mentioned in the preceding paragraph.

In this paper we will establish the stability of a large elliptical vortex in a disk (comparing to the disk size) against relaxation to a symmetrical state using neither of the above two methods with eigenanalysis and global maximum. The apparent contradiction between these results and those obtained by Briggs, Daugherty, and Levy [3] will be indicated due to the limitation of monotonic decreasing profiles in that paper. We will first deduce a stable sufficient condition from the conservation law of the Euler equation and the property of dynamical vorticity mixing. The energy of uniform vorticity will then be calculated (analytically at the small ellip-

\*Electronic address: peilong@toast.phy.ncu.edu.tw

ticity limit and numerically for general cases) and the vortices larger than a critical radius are shown to be stable from the comparison of energy. Testing the condition does not involve evaluating second derivatives, actually not even finding any equilibrium states. For smoothly distributed elliptical vortices, an approximating method is used and the results also suggest the existence of stable nonuniform ellipses. The robustness of these results under a small viscosity is also discussed. We further perform numerical simulations of the 2D Euler equation to test our predictions. Simulations not only confirm the sufficient condition, but also show that elliptical vortices are stable to much lower radii.

## II. THE STABILITY CONDITION

The stability condition used here can be summarized as follows. For an elliptical vortex at the center of a unit disk, if all possible symmetrical distributions obeying the global constraints (except energy) required by the Euler equation have energy less than that of the initial ellipse, this ellipse will never evolve to a symmetrical state.

Specifically, let us first consider a uniform-vorticity elliptical vortex with unit vorticity level sitting at the disk center. (Generalization to nonuniform vortices will be discussed later.) Now consider its possible dynamics toward an axisymmetrical vortex. This will be a state with a linear  $l=2$  diocotron mode if the vortex has an infinitesimal ellipticity.

The Euler equation conserves the total vorticity  $Q$ , angular momentum  $M$ , and energy  $E$  of the initial ellipse (the global constraints), which are given by

$$Q = \int \omega(\mathbf{r}) d\mathbf{r}, \quad M = \int r^2 \omega(\mathbf{r}) d\mathbf{r},$$

$$E_e = \frac{1}{2} \int \phi(\mathbf{r}) \omega(\mathbf{r}) d\mathbf{r}.$$

Furthermore, dynamical vorticity mixing ensures that the vorticity level of the resulting symmetrical vortex will never exceed one (the original uniform value). Under this restriction and given  $Q$  and  $M$  from the initial ellipse, there must be a maximum energy state with its energy denoted as  $E_s$  among all possible symmetrical distributions. Requiring conservation of energy, the condition then immediately follows:  $E_e < E_s$  is necessary for the ellipse to ever evolve to a symmetrical vortex;  $E_e > E_s$  is the *sufficient condition* for the ellipse *not* evolving to a symmetrical state. Applied to infinitesimal ellipticity, the  $l=2$  diocotron mode will not decay when  $E_e > E_s$ .

For general nonuniform vortices, first let us define  $G(\sigma)$  as the area covered by vorticity larger and equal to  $\sigma$ ,

$$G(\sigma) \equiv \int_V s(\omega(\mathbf{r}) - \sigma) d\mathbf{r},$$

with  $s(\sigma)$  the usual step function. Now dynamical vorticity mixing requires the inequality between  $G_e(\sigma)$  of the initial ellipse and  $G_s(\sigma)$  of the evolved symmetrical profile:  $G_e(\sigma) \geq G_s(\sigma)$ . Note that in the special case of uniform vorticity, this inequality is simplified to the previous statement about the vorticity not exceeding 1.

It should be noted here that this condition only attempts to exclude symmetrical states from possible evolutions, a limitation purely physically motivated. For example, it seems unlikely that an ellipse at the disk center will break the symmetry and relax to an off-center vortex, although we believe that the energy stability condition will not prohibit this dynamics. This conjecture (not decaying to off-center states) is consistent with numerical simulations in the tested parameter ranges which will be discussed in Sec. VI.

## III. SMALL ELLIPTICITY FOR UNIFORM VORTICES

Naturally we first want to examine the energy of uniform elliptical vortices, because of their large energy giving a better chance to satisfy the stability condition and the possible benefit on calculation due to their uniformness. We take a uniform elliptical vortex as a vorticity distribution  $\omega_e(\mathbf{r})$  in the polar coordinate  $(r, \theta)$ ,

$$\omega_e(r, \theta; r_0, \epsilon) = 1 - s(r - r_0(1 + \epsilon \cos 2\theta)), \quad (2)$$

with  $s(x)$  again the step function. The parameter  $r_0$  defines a base vortex size and  $\epsilon$  its ellipticity. The energy of this vortex in a unit disk can be written down using the Green function in a disk for the Poisson equation,  $\nabla^2 G(\mathbf{r}; \mathbf{r}') = -\delta(\mathbf{r} - \mathbf{r}')$ , with zero boundary condition at  $r=1$ . Using an opposite-charged image charge sitting at  $\mathbf{r}'' \equiv (1/r', \theta')$ , the Green function can be written as  $G(\mathbf{r}; \mathbf{r}') = -1/2\pi(\ln|\mathbf{r} - \mathbf{r}'| - \ln|\mathbf{r} - \mathbf{r}''| - \ln r')$ . The last term  $\ln r'$  is needed to give zero potential at  $r=1$ . The energy of the uniform elliptical vortex is then

$$E_e(r_0, \epsilon) = \frac{1}{2} \int \phi(\mathbf{r}) \omega(\mathbf{r}) d\mathbf{r}$$

$$= \frac{1}{2} \int_0^{2\pi} d\theta \int_0^{r_0(1 + \epsilon \cos 2\theta)} r dr$$

$$\times \int_0^{2\pi} d\theta' \int_0^{r_0(1 + \epsilon \cos 2\theta')} r' dr' G(\mathbf{r}; \mathbf{r}')$$

$$= E_0 + \int_0^{2\pi} d\theta \int_{r_0}^{r_0(1 + \epsilon \cos 2\theta)} r dr \phi_0(r; r_0)$$

$$+ \frac{1}{2} \int_0^{2\pi} d\theta \int_{r_0}^{r_0(1 + \epsilon \cos 2\theta)} r dr \int_0^{2\pi} d\theta'$$

$$\times \int_{r_0}^{r_0(1 + \epsilon \cos 2\theta')} r' dr' G(\mathbf{r}; \mathbf{r}'). \quad (3)$$

We separate  $E_e$  into three terms in the preceding equation. Here  $\phi_0(r; r_0)$  is the stream function of a uniform circular vortex with radius  $r_0$ ,  $(1/r)(d/dr)(r(d\phi_0/dr)) = -\omega_0$ ,  $\omega_0(r; r_0) = 1 - s(r - r_0)$ , and  $E_0$  its corresponding energy,

$$E_0 = \frac{1}{2} \int \phi_0(r; r_0) \omega_0(r; r_0) 2\pi r dr = \pi r_0^4 \left( -\frac{1}{4} \ln r_0 + \frac{1}{16} \right).$$

We know of no way to integrate Eq. (3) analytically. However, in this section we will calculate analytically the leading term in a small  $\epsilon$  expansion of  $E_e(r_0, \epsilon)$ , which is directly related to the linear stability of an  $l=2$  diocotron mode, and

in the next section we will present exact numerical results of  $E_e(r_0, \epsilon)$  with arbitrary  $\epsilon$ . Since the vortex is defined by  $r_0(1 + \epsilon \cos 2\theta)$ , the lowest order dependence on  $\epsilon$  must be  $\epsilon^2$ . Correct to the order of  $\epsilon^2$ , the second term in Eq. (3) is quickly found to be

$$\begin{aligned} & \int_0^{2\pi} \frac{1}{2} [r_0 \phi_0'(r_0; r_0) + \phi_0(r_0; r_0)] r_0^2 \epsilon^2 \cos^2 2\theta d\theta \\ &= -\frac{1}{4} \pi r_0^4 (1 + \ln r_0) \epsilon^2. \end{aligned}$$

Here the prime denotes the derivative respected to  $r$ . Evaluation of the third term in Eq. (3) is more difficult. Again correct to the order of  $\epsilon^2$ , the integration becomes

$$\frac{1}{2} r_0^4 \epsilon^2 \int_0^{2\pi} d\theta \int_0^{2\pi} d\theta' \cos 2\theta \cos 2\theta' G(r_0, \theta; r_0, \theta').$$

Using the Green function and changing to new variables  $u \equiv \theta + \theta'$  and  $v \equiv \theta - \theta'$ , after some algebra, we reach

$$\frac{1}{8} r_0^4 \epsilon^2 \left[ \pi + \int_0^{2\pi} \ln(a - \cos v) \cos 2v dv \right] \equiv I_a, \quad (4)$$

with  $a \equiv \frac{1}{2}(r_0^2 + 1/r_0^2) \geq 1$ . The integration  $I_1 \equiv \int_0^{2\pi} \ln(1 - \cos v) \cos 2v dv = -\pi$  has also been used in reaching Eq. (4).

The integration in Eq. (4) is computed by first integrating  $\partial I_a / \partial a$ , and then using  $I_1$  to determine the constant arising from integration of  $a$ . Eventually Eq. (4) is found to be  $\frac{1}{8} \pi r_0^4 (1 - r_0^4) \epsilon^2$ , and the energy of the elliptical vortex becomes

$$E_e(r_0, \epsilon) = E_0 + \frac{1}{4} \pi r_0^4 \left( -\frac{1}{2} r_0^4 - \frac{1}{2} - \ln r_0 \right) \epsilon^2 + O(\epsilon^4). \quad (5)$$

The energy  $E_e(r_0, \epsilon)$  is now to be compared with the energy  $E_s$  of the maximum-energy symmetrical state with the same values of total vorticity  $Q$  and angular momentum  $M$ . Its vorticity must also be equal to or less than 1. To see what this state is, first it is favorable to have all the vorticity stay together, i.e., a uniform unit-valued circular vortex with radius  $r_s = (Q/\pi)^{1/2}$ , to gain as much as energy. However, this circular vortex has a fixed angular momentum  $\frac{1}{2} \pi r_s^4$ , and the uniform ellipse always has a larger value. To satisfy the requirement of both  $Q$  and  $M$ , as well as achieving a maximum energy, the vorticity distribution  $\omega_s(r)$  will be

$$\omega_s(r) = \begin{cases} 1 & \text{for } 0 < r < \alpha \text{ and } \beta < r < 1 \\ 0 & \text{for } \alpha < r < \beta. \end{cases} \quad (6)$$

Here  $\alpha$  and  $\beta$  depend on  $Q$  and  $M$ , which are determined by  $r_0$  and  $\epsilon$ . In this profile, a certain amount of vorticity is put as far away from center as possible, i.e., at the disk boundary, to account for the excess angular momentum, and a maximum amount of vorticity is left to concentrate at the center to acquire a maximum energy [12]. Here we see how the system size comes into play in a delicate manner. At small  $\epsilon$ ,  $\alpha = r_0 [1 + \frac{1}{4}(1 - 3r_0^2/1 - r_0^2) \epsilon^2]$  and  $\beta = 1 - \frac{1}{2}(r_0^4/1$

$-r_0^2) \epsilon^2$ , and the energy  $E_s$  is expanded as (it involves only straightforward algebra to solve  $\phi_s$  and then integrate  $E_s$ )

$$E_s = E_0 - \frac{1}{4} \pi r_0^4 \frac{1 - 3r_0^2}{1 - r_0^2} \ln r_0 \epsilon^2 + O(\epsilon^4).$$

Now we obtain the energy difference between  $E_e$  and  $E_s$  as

$$E_e - E_s = \frac{\pi}{4} r_0^4 \left( -\frac{1}{2} r_0^4 - \frac{1}{2} - \frac{2r_0^2}{1 - r_0^2} \ln r_0 \right) \epsilon^2 + O(\epsilon^4).$$

Evaluation of the  $\epsilon^2$  term reveals that there is a critical value of  $r_0$  at  $r_c = 0.586$  such that  $E_e < E_s$  for  $r_0 < r_c$  and  $E_e > E_s$  for  $r_0 > r_c$ .

So applying the energy condition, this indicates that the  $l=2$  mode perturbation of a uniform circular vortex in a finite disk will not decay if the vortex is large enough (larger than 0.586 times the disk radius). This result seems to contradict that of Briggs, Daugherty, and Levy [3], where decaying modes were calculated from eigenanalysis for all  $l \geq 2$  modes of a circular vortex with a smooth profile very close to  $\omega_0(r; r_0)$  (a step at  $r_0$ ) but with negative  $\omega'(r)$  at all  $r$ . The resolution is that in the calculation of Briggs, Daugherty, and Levy, the symmetrical vortex is assumed as a monotonic decreasing function of  $r$ . This seems a reasonable and harmless condition. However, as Eq. (6) shows, this condition is very restrictive and always violated by uniform ellipses and hence their results no longer apply.

#### IV. UNIFORM VORTICES WITH ARBITRARY ELLIPTICITY

In this section we treat general ellipticity cases by computing numerically the energy of uniform vortices defined by Eq. (2) with arbitrary  $\epsilon$ . Let us first consider the possible effects at a large ellipticity. When  $\epsilon$  increases at a fixed  $r_0$  in Eq. (2), the energy will decrease at the same time the angular momentum rises. Larger angular momentum also results in a smaller energies of the corresponding symmetrical vortex, as more vorticity will stay outside. Since both energy are decreasing, we cannot tell before the calculation of exact values whether a larger ellipticity will make the energy condition more easily satisfied or not.

To numerically calculate  $E_e(r_0, \epsilon)$  of uniform elliptical vortices with arbitrary  $\epsilon$ , we use another form of the Green function since that using image charges in the preceding section has logarithmic functions and is not easy to handle numerically. The Green function is now written as a summation of Fourier components in the azimuthal direction,

$$G(\mathbf{r}; \mathbf{r}') = \sum_{m=0}^{\infty} g_m(r; r') \cos[m(\theta - \theta')],$$

with  $g_m$  functions of both  $r^{\pm m}$  and  $r'^{\pm m}$ . The energy now becomes a summation on  $m$  of four-dimensional  $(r, \theta, r', \theta')$  integrals. The integration on  $r$  and  $r'$  can be carried out analytically and the energy simplifies to a summation of double integrals on  $\theta$  and  $\theta'$ . The integrals are then calculated numerically, and results are checked to conform to Eq. (5) at small  $\epsilon$ .

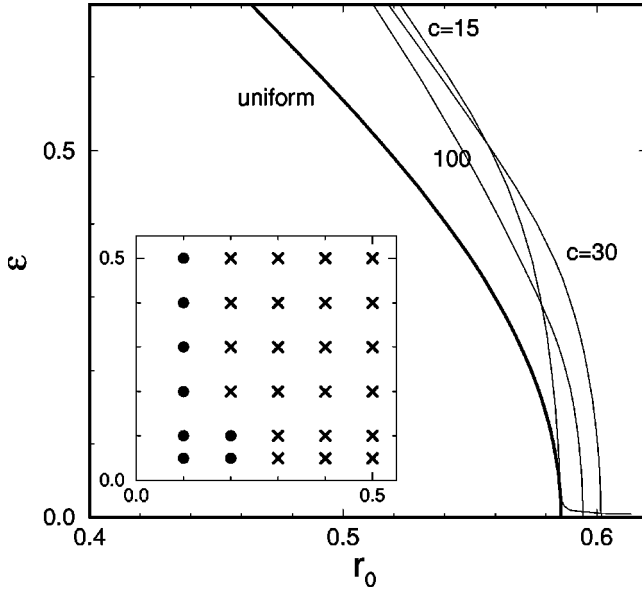


FIG. 1. The vortex size and ellipticity space. The thick line is the stable critical radius for uniform vortices. The thin lines are for smooth vortices with  $c=100$ ,  $30$ , and  $15$ , and calculated by conserving  $Z_4$ . In the inset, crosses represent relaxations to elliptical states in simulations, and circles to symmetrical states.

The exact value of  $E_e(r_0, \epsilon)$  now enables us to establish the stability of finite ellipticity at uniform vorticity. In Fig. 1 of the  $r_0$ - $\epsilon$  plane, we plot a thick line indicating the position where  $E_e = E_s$ . (Although complicated, again  $E_s$  with arbitrary  $\epsilon$  can be written down analytically from straightforward algebra.) To the right of the line,  $E_e > E_s$  and an elliptical vortex will never relax to a symmetrical vortex. The curve crosses  $\epsilon = 0$  at  $r_0 = 0.586$ , the value we have obtained from the small  $\epsilon$  expansion. As  $\epsilon$  is increased, the critical radius where  $E_e = E_s$  becomes smaller, indicating a stronger effect from increasing angular momentum than decreasing energy. To the left, the present analysis only says that the decay to a symmetric state is allowed, but its occurrence is not implied.

It should be emphasized here that we have proved that the ellipse defined by Eq. (2) will not decay to a symmetrical state if  $r_0 > r_c$ . It is very likely that dynamically it will undergo adjustment and reach an elliptical-like steady state. We cannot say about its exact distribution. It probably should be a state described by  $\omega(\mathbf{r}) = \omega[\phi(\mathbf{r}) + \Omega r^2]$ , with  $2\Omega$  giving the rigid body rotation frequency around the disk center. Given a particular assumption on this functional dependence, an exact distribution can then be computed. One example is the mean field equilibrium [10]. However, whether and when the system will reach the prediction from this maximum-entropy principle (thermal equilibrium) is still not very clear [14].

We should have some discussions here about the effect of viscosity, which is always present in real physical situations, on the elliptical vortices. Ignoring the issues of all other quantities, the system energy will gradually decrease due to the viscous dissipation and an original stable ellipse with an energy larger than  $E_s$  could hence relax to a symmetrical state after its energy falls below  $E_s$ . However, the finite difference between the initial  $E_e$  and the symmetrical  $E_s$  makes this happen in a viscous time scale which is going to

be very large at a small viscosity comparing to the time scale of inviscid processes. What we are interested in here is the dynamical behaviors in these rapid inviscid processes and the presence of a small viscosity should not have large effects. This separation of time scale is well documented in various experiments and simulations [13] and could also be seen in our simulations (Sec. VI).

## V. NONUNIFORM VORTICITY ELLIPSES

In the previous sections the energy of both uniform elliptical and symmetrical vortices is calculated to obtain the stable critical radii. We now want to discuss elliptical vortices with smoothly distributed vorticity. Consider the situation when the edge of a uniform vortex becomes smeared; the energy should change gradually (not discrete jump) with the degree of “smoothness.” Thus we should be able to say that smoothly distributed ellipses close to uniform vortices still have stable critical radii. To quantitatively compute the critical radii now, however, is not easy, and it is not clear whether smooth vortices far away from uniform could remain stable. The energy of nonuniform, smoothly distributed ellipses (which we will define as some particular distributions) is actually easier to compute numerically than the uniform cases by using a two-dimensional grid with enough grid points. However, the energy of the corresponding maximum-energy symmetrical profiles is very difficult to obtain, as there is this functional constraint  $G(\sigma)$ . Hence in this section we will only present an approximating method to test the stability condition. The purpose of this calculation is then to demonstrate that there should still be stable smooth elliptical vortices, not to obtain exact values of the critical radii.

The maximum-energy symmetrical profiles now should have the same  $G(\sigma)$  as the initial ellipse. In real implementation, we can require the quantities  $Z_n, n=1,2,3, \dots$ , defined by

$$Z_n \equiv \int_V \omega^n(\mathbf{r}) d\mathbf{r},$$

to be conserved. In the special case of uniform ellipses, the symmetrical states are also uniform, as we have done in the previous sections. For the general case, however, it becomes a highly nontrivial task to find this maximum-energy state.

We use the smooth elliptical vortices defined in the polar coordinate by,

$$\omega(\mathbf{r}) = \frac{1}{1 + \exp\{c[r - r_0(1 + \epsilon \cos 2\theta)]\}}. \quad (7)$$

Here again  $r_0$  gives a base vortex size,  $\epsilon$  its ellipticity [cf. Eq. (2)], and  $c$  the smoothness near the edge. In Fig. 2, we show  $\omega(r; r_0=0.5, \epsilon=0)$  with three different values of  $c$  (100, 30, 15).

The energy of these vortices is calculated using a polar coordinate grid inside a unit circle. The Poisson equation,  $\nabla^2 \psi = -\omega$ , is solved by Fourier expansion in the azimuthal direction. Radial equations are thus decoupled for different Fourier modes and they are solved by a fourth-order finite difference method. Calculations in various numbers of grid



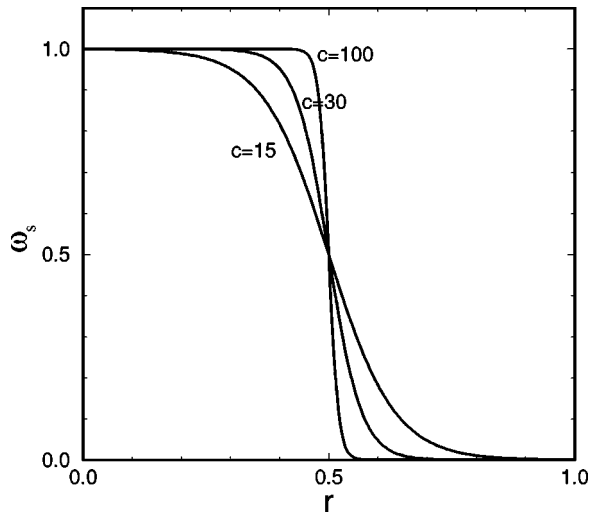


FIG. 2. Plot of vorticity distribution Eq. (7) with  $r_0=0.5$ ,  $\epsilon=0$ , and three different values of  $c$ .

points are done to make sure enough accuracy is achieved. That usually means up to the grid of  $1024 \times 1024$ .

We then use the following distribution to approximate the corresponding symmetrical state:

$$\omega(r) = \frac{1}{1 + \exp[c'(r - \alpha)]} + \frac{1}{1 + \exp[c'(\beta - r)]}. \quad (8)$$

This form is motivated by Eq. (6) with additional smoothing controlled by  $c'$ . With three parameters ( $\alpha, \beta, c'$ ), this equation can satisfy, besides  $Q$  and  $M$ , only a particular choice of  $Z_n$  from the initial elliptical vortex, as oppose to all  $Z_n$  as required by the exact stability condition. So results thus calculated should be treated cautiously.

Nevertheless, in Fig. 3 we show the calculated critical radii for  $c=100$  with several different  $Z_n$  as the constraint. The curves are again obtained by comparison between the energy of states from Eqs. (7) and (8) and mark where these two energy are equal. Although different choices of  $Z_n$  give different curves of critical radii, we believe they nonetheless

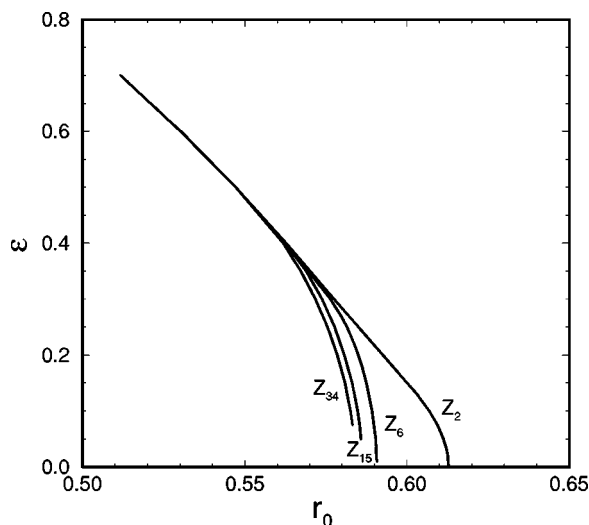


FIG. 3. Critical radii for smooth vortices with  $c=100$  and using different  $Z_n$  as the constraints.

hint at the existence of critical radii for stable ellipses at some places. Especially at large  $\epsilon$ , they are almost approaching a single curve. The reason we believe this is as follows. A significant portion of the increased angular momentum at small  $\epsilon$  should be accounted for by adjusting the vorticity distribution near the edge and this adjustment is strongly affected by the particular choice of constraint  $Z_n$ . Hence different critical radii in Fig. 3 at small  $\epsilon$ . However, at large  $\epsilon$ , most of the excess angular momentum must be achieved by putting enough vorticity at the disk boundary, as in the previous uniform case. The adaption is largely determined by  $Q$  and  $M$ , leading to a single curve for different  $Z_n$  at large  $\epsilon$ .

In Fig. 1, we plot three additional thin lines marking the critical radii calculated for  $c$  equal to 100, 30, and 15, with  $Z_4$  as the choice of constraint. These thin lines calculated from the above approximation we believe suggest that large smooth elliptical vortices are also stable, like the stable uniform ellipses we have proven in the previous sections. Different choices of  $Z_n$  gives qualitatively similar results. Finally, we note that at  $c=15$  the behavior very close to  $\epsilon=0$  seems to indicate that linear elliptical vortices will not satisfy the stability condition. However, we should bear in mind the approximating nature of the calculations for these thin lines.

## VI. NUMERICAL SIMULATIONS

We have performed numerical simulations to test our predictions. Simulations of the Euler equation in the polar coordinate have the difficulty of singularity at the origin due to vanishing grid spacing. To avoid this singularity, we use the functions

$$x = \mu \sqrt{1 - \zeta^2/2},$$

$$y = \zeta \sqrt{1 - \mu^2/2},$$

mapping a unit disk in the  $x$ - $y$  plane to a square in the  $\mu$ - $\zeta$  plane with  $-1 \leq \mu \leq 1$  and  $-1 \leq \zeta \leq 1$ . The simulation is then done in the  $\mu$ - $\zeta$  plane with a Cartesian coordinate. The resolution is mostly  $256 \times 256$ , with a few  $512 \times 512$  runs to test convergence. By avoiding the polar coordinate and hence the singularity at the origin, we need only a very small numerical viscosity term,  $\nu \nabla^2 \omega$ , to stabilize the simulation. The viscous time scale hence becomes very large and our results of inviscid relaxation behaviors can then be independent of the viscosity. The second-order finite difference is used for spatial derivatives. Temporally the second-order explicit Adams-Bashford scheme is used for the nonlinear term and the fully implicit scheme is used for the viscous term.

Distributions defined by Eq. (7) with  $c=30$  are used as our initial conditions. For an initial ellipse with particular values of  $r_0$  and  $\epsilon$ , we run simulations to a long time and determine whether their final states are elliptical or symmetrical. The results are plotted in the inset of Fig. 1 as symbols, where crosses indicate relaxation to elliptical states and solid circles to symmetrical states. There are no results at very small  $\epsilon$  as very high resolutions are needed to resolve differences between elliptical major and minor axes at this limit. In the figure we see the confirmation of the predictions from the stability condition, namely the stable elliptical vor-

tices with large vortex sizes. We note that no relaxations to off-center vortices have happened.

The simulations also show that ellipses are actually stable to lower radii. This can be reasonably explained by the dynamical behavior of the ellipses observed in the simulations. Generically, an initial ellipse will shed some vorticity in the form of vorticity filaments toward the disk boundary and the center vortex either reaches a distribution with a smaller ellipticity or becomes symmetric. However, these filaments seldom really reach the disk boundary, as opposed to the extreme situation at the calculation of the energy of the maximum-energy symmetrical state. In other words, these filaments do not carry away the maximum possible angular momentum, leading to elliptical vortices at the center.

## VII. SUMMARY

In conclusion, we have shown that, from the requirement of vorticity mixing in dynamical evolution and energy con-

servation, large elliptical vortices in a finite disk will remain stable. At the infinitesimal ellipticity limit, this indicates stable  $l=2$  diocotron modes for large vortices. The critical radii for uniform vortices is rigorously computed. The existence of stable smooth vortices are also suggested by an approximating calculation. Numerical simulations not only confirmed these results, but also show that elliptical states are actually stable to a smaller size. The contradiction to the current general idea of decaying  $l=2$  modes is also indicated due to the incompleteness of considering only monotonic decreasing vorticity by Briggs, Daugherty, and Levy.

## ACKNOWLEDGMENTS

The author thanks Dr. C. Y. Lu for fruitful discussions and C. R. Lo for the help with the numerical simulations. The support of National Science Counsel, Taiwan, through Contract No. NSC 87-2112-M-008-034, is also acknowledged.

- 
- [1] R. H. Levy, *Phys. Fluids* **8**, 1288 (1965).
  - [2] H. Lamb, *Hydrodynamics*, 6th ed. (Dover, New York, 1932), Secs. 158, 159.
  - [3] R. J. Briggs, J. D. Daugherty, and R. H. Levy, *Phys. Fluids* **13**, 421 (1970).
  - [4] N. S. Pillai and R. W. Gould, *Phys. Rev. Lett.* **73**, 2849 (1994).
  - [5] T. B. Mitchell and C. F. Driscoll, *Phys. Rev. Lett.* **73**, 2196 (1994).
  - [6] Please see D. D. Holm, J. E. Marsden, T. Ratiu, and A. Weinstein, *Phys. Rep.* **123**, 1 (1985) for a review. See also P. J. Morrison, *Rev. Mod. Phys.* **70**, 467 (1998).
  - [7] R. C. Davidson and S. M. Lund, *Phys. Fluids B* **3**, 2540 (1991).
  - [8]  $\omega$  and  $\phi$  here actually should be defined in a rotating frame.
  - [9] T. M. O'Neil and R. A. Smith, *Phys. Fluids B* **4**, 2720 (1992).
  - [10] J. Miller, *Phys. Rev. Lett.* **65**, 2137 (1990); R. Robert and J. Sommeria, *J. Fluid Mech.* **229**, 291 (1991); J. Miller, P. B. Weichman, and M. C. Cross, *Phys. Rev. A* **45**, 2328 (1992).
  - [11] See, e.g., P. Chen and M. C. Cross, *Phys. Rev. E* **54**, 6356 (1996).
  - [12] Here we have not given a rigorous proof of the maximum-energy symmetrical state. Please see Ref. [11] for more discussions about this state.
  - [13] See, e.g., M. V. Melander, N. J. Zabusky, and J. C. McWilliams, *J. Fluid Mech.* **195**, 303 (1988); K. S. Fine, C. F. Driscoll, J. H. Malmberg, and T. B. Mitchell, *Phys. Rev. Lett.* **67**, 588 (1991); also [4].
  - [14] See, e.g., P. Chen and M. C. Cross, *Phys. Rev. Lett.* **77**, 4174 (1996), and references therein.